Supporting Information

Tafvizi et al. 10.1073/pnas.1016020107

SI Text

DNA Preparation and Flow Stretching. Purified DNA from λ phage (New England Biolabs) was linearized and biotinylated at one end by annealing a 3′ biotin-modified oligo (5′AGGTCGCCG-CCC3′-biotin; Integrated DNA Technologies) to the complementary λ-phage 5′ overhang. Flow cells (0.1 mm height, 2.0 mm width) with a streptavidin-coated surface were prepared as described previously (1–3). The streptavidin-coated flow-cell surfaces were blocked by incubation with blocking buffer (Tris 20 mM, EDTA 2 mM, NaCl 50 mM, BSA 0.2 mg/mL, Tween 20 0.005%; pH 7.5) for 20 min. Biotin-modified DNA constructs were introduced into the flow cell at a rate of 0.1 mL/min at a concentration of 10 pM for 20 min. These conditions resulted in an average density of ∼100 surface-tethered DNA molecules per field of view ($\sim 50 \times 50\ \mu m^2$).

The single-molecule imaging experiments were performed in an imaging buffer, containing 20 mM Hepes, 0.5 mM EDTA, 2 mM $MgCl_2$, 0.5 mM DTT, 0.05 mg/mL BSA (pH 7.9), and varying amounts of KCl. Imaging buffer was drawn into the channel by a syringe pump at a flow rate of 0.1 mL/min, creating shear flow near the coverslip surface (4). Single-molecule imaging was done with 30–100 pM TC (Tetramerization + C-terminal) p53 and 10–50 pM NCT (N-terminal + Core domain + Tetramerization) in imaging buffer. The proteins were kept at low-micromolar concentration, and were diluted right before the single-molecule experiment. The single-molecule experiments were done within less than 1 h from the time of dilution. Due to the slow kinetics of the tetramer-dimer transition (5), all constructs are assumed to be in the tetrameric form during the single-molecule experiment.

Protein Preparation and Labeling. ***Expression and purification of TC.*** P53 Tet + C (293–393) with an N-terminal cysteine was cloned in PET 24-HLTev using BamHI and EcoRI sites. The resulting plasmid encodes a fusion protein with an N-terminal 6xHis tag, followed by a lipoyl domain, a TeV protease cleavage site, and the p53 Tet + C (293–393) sequence of interest. The proteins were expressed in *Escherichia coli* strain BL21 and purified by a Ni-affinity column followed by cleavage with TeV overnight. Subsequent purification by cation exchange chromatography on SP Sepharose and gel filtration on Superdex 75 yielded a purity of >99% (6). To measure the oligomerization state of the TC domain, we measured the lifetime of different TC domains as well as only the C-terminal domain on DNA. The average lifetime of the C-terminal domain on DNA is 0.88 ± 0.05 seconds, whereas the TC domain has the lifetime of 2.41 ± 0.08 seconds on DNA. Both experiments are done in 25 mM total salt concentration. Because the tetramerization domain does not interact with DNA, we conclude than the TC domain in our single-molecule experiment conditions must be a dimer or tetramer.

Labeling of TC. The labeling was carried out in phosphate buffer (20 mM sodium phosphate, 150 mM NaCl, pH 7.0) with a protein concentration of 100 μM on ice. 10-fold excess Alexa Fluor 555 maleimide was added in the presence of 1 mM of tris(2-carboxyethyl) phosphine (TCEP). The labeling progress was followed by matrix assisted laser desorption/ionization time-of-flight mass spectrometry (MALDI-TOF MS). The reaction was quenched with 10 mM β-mercaptoethenol after ∼1 h. The mixture was then loaded onto a G-25 desalting column to separate excess dye.

Purification and labeling of NCT. The superstable mutant of NCT p53 (N-terminal + core domain + Tetramerization domain, residues 1–363) with mutations M133L, V203A, N239Y, and N268D (7) was used. The protein was expressed in *Escherichia coli* and purified as described (6, 8).

The NCTwas labeled with Alexa Fluor 555 carboxylic acid succinimidyl ester (Invitrogen) through the N terminus amine. The labeling was carried out in phosphate buffer (50 mM sodium phosphate, 150 mM NaCl, pH 6.4). Alexa Fluor 555 of equal molarity was added to 1 mL of NCT solution (30 μM). The labeling progress was followed by MALDI-TOF MS. The reaction was quenched after about 1 h with 0.2 mL of 1 M Tris (hydroxymethyl) aminomethane-HCl (pH 7.4) and the labeled protein was separated from the free dye on a G-25 desalting column.

Fluorescence Imaging. Fluorescence imaging of the movement of the labeled p53 proteins and its different domains along DNA was performed by placing the flow cell on top of an inverted microscope (Olympus IX71) and exciting the AlexaFluor 555 label by the 532-nm line of a frequency doubled, Nd:YAG laser (Crystal laser, GCL-100-M) with 100 mw maximum output. A high-N.A. microscope objective (Olympus, 60×1.6x/1.45 N.A.) was used to illuminate the sample with total-internal reflection. The illuminated area had a diameter of 50 μm at the sample plane. The fluorescence was collected by the same objective and imaged by an EM-CCD digital camera (Hamamatsu C9100-13), after filtering out scattered laser light. The movies were recorded by MetaVue imaging software.

Particle Tracking. The positions of labeled particles were determined by fitting each single-molecule fluorescence image to a two-dimensional Gaussian distribution. We calculate the standard error of position determination to be $\sigma = 10$–20 nm (3).

The trajectories of the particles were then tracked by custom-written particle-tracking MATLAB code. The trajectories were further analyzed to measure the drift and diffusion coefficient of each protein in the population (3).

Site-Specific Labeling of Biotin-Lambda. We use a previously published protocol (9, 10) to site-specifically label the biotin-lambda DNA at 14,725 base-pairs from the tethered point. Treatment of biotin-lambda DNA with the sequence-specific Nt.Bst.NBI nicking endonuclease results in single-strand breaks corresponding to the recognition site of the enzyme. Some of the nicks occur closely spaced and on the same strand. The oligonucleotides between closely spaced nicks can be replaced with modified oligonucleotides of the same sequence via a strand-displacement reaction and subsequent ligation. Nicking reactions with Nt.Bst.NBI (NEB, 20 units) were performed on biotin-lambda DNA (2.5 μg) at 50 °C for 2 h in buffer 3 (NEB). The nicked DNA was mixed with 100-fold excess of a 13-base oligonucleotide (IDT) modified with a 5′ digoxigenin (5′-digoxigenin-TTCA-GAGTCTGAC-3′), heated at 50 °C for 10 min and then slowly cooled to room temperature, resulting in the highly efficient replacement of the native sequence. Ligation was performed for 2 h at room temperature using T4 ligase. At the end, the activity of the nicking enzyme was quenched by adding 20 mM EDTA. The digoxigenin was detected by flowing in and then washing out a solution of 1 nM quantum dots (QDot; Invitrogen) which were functionalized with antidigoxigenin Fab fragment (Roche) using the Invitrogen QDot Antibody Conjugation Kit. The DNA was

stretched and the QDot fluctuations characterized using the same flow conditions as described in the p53 experiments.

Determination of Drift Rates. We measure the presence of any directional bias in the protein motions caused by the flow of the buffer by measuring the total displacement of all protein trajectories divided by the total duration of all trajectories. In the absence of any drift, the net displacement per time unit for a population of proteins is a normal distribution around zero. However, in the presence of buffer flow, a drag force will be exerted on the protein and will force it to move in the direction of the flow. Therefore, the net displacement of the population of proteins is shifted in the direction of the flow. To take into account the fact that trajectory lengths are different for every measured protein, we measure the weighted drift of our protein populations as follows:

$$\text{drift}_{\text{mean,weighted}} = \frac{\sum_{i=1}^{N} l_i d_i}{\sum_{i=1}^{N} l_i},$$

where l_i is the length of trajectory I and d_i is the measured drift for that trajectory. The variance of all the trajectories in one biochemical condition can likewise be calculated by:

$$\sigma^2{}_{\text{weighted}} = \frac{\sum_{i=1}^{N} l_i (d_i - \text{drift}_{\text{mean,weighted}})^2}{\sum_{i=1}^{N} l_i}.$$

The error bars can be calculated as $\frac{\sigma}{\sqrt{N}}$ where N is the total number of trajectories in that biochemical condition. Fig. S1 shows the drift histogram for core and C-terminal domain in 75 mM total salt concentration for 385 and 183 trajectories respectively. The drift for core domain is almost centered around zero, resulting in a small mean of 6.1 ± 7.6 nm/seconds. The weighted mean of drift for C-terminal domain is 355.8 ± 98.4 nm/seconds. A similar distribution of drift is observed for other salt concentrations.

Calculating Diffusion Coefficient by Minimizing the Effect of DNA Fluctuations. To calculate the diffusion coefficients for the different p53 constructs while minimizing the impact from DNA fluctuations, we only fit the portion of the Mean Square Displacement (MSD) plot between 0.25 to 0.5 s, a region in which the MSD of the DNA fluctuations is constant and does not contribute to the diffusion coefficient (3). Furthermore, we exclude trajectories obtained from proteins on the one-third of the DNA farthest from the tether point (between 33,777 and 48,502 bp), as the underlying DNA fluctuations become too large compared to the diffusion coefficient to extract reliable diffusional properties (Fig. S2). The histogram of diffusion coefficient for different constructs of p53 are shown in Fig. S3.

Three-Dimensional Diffusion Coefficient of Different Domains. The diffusion coefficient for a spherical object diffusing by purely translational movement in one dimension can be calculated by the Stokes-Einstein relation:

$$\text{D}_{3d} = \frac{k_{\text{B}} T}{6\pi\eta a}.$$

Where η is the solvent viscosity (8.9×10^{-4} Pa·s for water at 25 °C), a is the radius of the diffusing tetrameric p53 protein (4.9 nm) (3), k_{B} is the Boltzman constant, and T is the temperature. For tetrameric p53 in our experimental conditions, this calculation results in a three-dimensional diffusion coefficient of 4.8×10^7 nm^2/seconds. The diffusion coefficient of the TC (Tetramerization + C-terminal domain) and NCT (N-terminal + Core + Tetramerization domain) can as well be calculated using the molecular weight of these domains, which results in 4.9×10^7 nm^2/seconds and 7.5×10^7 nm^2/seconds for NCT, and TC domains respectively.

Residence Time of Core Domain on DNA. The salt dependence of the diffusion coefficient of the core domain implies a hopping mechanism for diffusion of the core domain on DNA. The core domain therefore translocates on DNA by undergoing microscopic association and dissociations on and off the DNA. Upon dissociation, the protein will diffuse a short distance in solution, resulting in rebinding to the DNA at a different position. During these brief excursions into solution, the protein will also experience a small hydrodynamic drag from the buffer flow, resulting in the drift of the C-terminal truncated protein. The dependence of the diffusion coefficient of the core domain on salt concentration can be rationalized by the amount of the time that the protein spends in solution. At higher salt concentration, the protein spends longer time in solution, resulting in the increase of diffusion coefficient of core domain. The fraction of time that the protein spends in solution can be determined by comparing our observed experimental diffusion coefficient with that obtained for a protein freely diffusing in solution. For the NCT domain, the diffusion coefficient in solution is 4.9×10^7 nm^2/seconds and the experimental diffusion coefficient is measured to be $(2.39 \pm 0.48) \times 10^4$ nm^2/seconds (at 75 mM total salt concentration). These values suggest that the core domain spends only 10^{-4}–10^{-3} of the total time in solution and thus is bound to the nonspecific DNA the majority of the time (>99.9%).

Measuring the Time That Core Domain Spends in Solution Based on Drift. The velocity of buffer at the DNA can be estimated using the flow rate of the buffer and the dimensions of the channel. In our flow-stretching assay, the buffer solution was drawn into the channel by a syringe pump with a flow rate of 0.1 mL/ min creating a shear flow near the coverslip surface. The flow channel is 100 μm in height and 2 mm in width, which results in the average velocity of 0.83 cm/ sec for the buffer in the channel. The flow velocity, however, is not a constant throughout the channel, but is zero at the boundaries, yielding a parabolic flow profile (3). The mean distance of the DNA from the coverslip surface is 0.2 μm (3, 4, 11). With a channel height h, the flow velocity v_y at a distance y from the surface can be expressed as:

$$v_{\text{avg}} = \frac{2}{3} v_{\text{max}} \quad \text{and} \quad v_y = v_{\text{max}} \left[\frac{hy - y^2}{h^2/4}\right] = \frac{3}{2} v_{\text{avg}} \left[\frac{hy - y^2}{h^2/4}\right].$$

The average velocity of the flow at the center of the DNA, 0.2 μm above the surface, can be estimated as 100 μm/ sec. Assuming that the core domain only moves when it is dissociated from the DNA, the drift of the core domain can be estimated as the product of the ratio of the time it spends in the solution and the velocity of the buffer at the DNA. Measured from the diffusion coefficient, the core domain spends only 10^{-4}–10^{-3} of the total time in solution and thus is bound to the nonspecific DNA the majority of the time (>99.9%). The small time spent in solution will result in drift of about 10 nm/ sec which is within the error bar of the observed experimental drift.

Comparing the Ruggedness of Energy Landscape of Translocating Along DNA for Different p53 Domains and Their Affinity to Nonspecific DNA. Difference in the ruggedness of the sequence-specific energy landscape between the core and C-terminal domains is also consistent with different affinities of these domains to nonspecific DNA. Theory (12) gives the residence time of a domain on DNA as

$$\tau_{1D} \sim \exp(E_{ns}/k_BT + \sigma^2/(2(k_BT)^2),$$

where $E_{ns} > 0$ is the free energy difference for the protein to be in the solvent and on DNA, and σ is the measure of the landscape ruggedness. This estimate predicts that sequence-specific core domain (large σ) spends more time on nonspecific DNA as compared to the C-terminal domain. Consistent with this argument the Kd for nonspecific DNA for C-terminal (Tet + C-terminal) and core domain (Tet + Core) are several μM and 680 nM respectively (6, 13). These numbers show a higher affinity for the core domain to nonspecific DNA compared to the C-terminal domain. We observed a similar behavior in our single-molecule experiments. While the lifetime of the core domain constructs on DNA is very long (several minutes, limited by photo-bleaching), the TC domain is very short lived on DNA (about 3 s for TC, Fig. S4). This shows that the affinity of the core domain to the nonspecific DNA is higher than that of the C-terminal domain.

Energy Barriers of Translocation for C-Terminal Domain and Core Domain. The energy barriers of translocation for the sliding of core domain and C-terminal domain can be calculated by comparing the measured experimental diffusion coefficient and the maximum rotational diffusion coefficient for TC and NCT domains by (12):

$$D_{exp} = D_{theor,lim}(1 + \sigma^2\beta^2)^{1/2} \exp(-7\sigma^2\beta^2/4).$$

This calculation results in a roughness of the energy of 0.6 k_BT for C-terminal domain and 2.3 k_BT for core domain sliding along DNA. The slow diffusion of core domain, which is the sequence-specific domain of p53, on DNA is consistent with theory where sequence specificity requires high variance ($\sigma > 2\ k_BT$) of the energy landscape. Also the rapid diffusion of C-terminal domain, which nonspecifically binds DNA, is consistent with theory where small roughness of the energy landscape ($\sigma < k_BT$) is required for fast search (12) (Fig. S5). The full-length p53 requires both fast search and sequence-specificity for the target site and its diffusion can be explained in the context of a two state model (See main text).

Estimates for p53 Search Process. ***Fraction of time in the search state.*** Diffusion of the full-length p53 is slower than that of the C terminus due to two factors: (*i*) difference in the size of the protein; (*ii*) some fraction of time spent in the immobile recognition conformation:

$$D_{fl,exp} = \gamma \cdot f \cdot D_{Cterm,exp},$$

where γ is the ratio of the rotational diffusion coefficient of the two proteins, and f is the fraction of time spent in the search state. Recently the quaternary structure of p53 on the cognate DNA site has been solved by a combination of small-angle X-ray scattering and NMR (14). The structure shows that the core domains are in close contact with the DNA, while the tetramerization domains form the most remote region of the structure on the other side of DNA. C-terminal domains have not been resolved (must be disorder) but are likely to interact with nonspecific DNA on the same side as the tetramerization, i.e., opposite of the core domains. We estimate the difference in the theoretical limit of the rotational diffusion coefficient between the TC (tetramerization and C-terminal domain) construct (293–393 = 100 aa) and the fl p53 (393 aa). The upper limit of the rotational diffusion coefficient can be calculated by:

$$D_{lim} = \frac{k_BT}{\xi}.$$

Where ζ is the total friction of the protein rotating along the DNA helix and can be calculated by (15):

$$\zeta = 6\pi\eta R + \left(\frac{2\pi}{10BP}\right)^2 [8\pi\eta R^3 + 6\pi\eta R(R_{OC})^2]$$

for a protein with radius R and distance R_{OC} from DNA. From Fig. S6, for the full-length p53 the total friction is the sum of the frictions of the tetramerization domain with radius r and distance r_{oc} from DNA and the core domain with radius R and distance R_{OC} from the DNA. The ratio of the upper limit of rotational diffusion for TC domain and full-length p53 can be calculated as:

$$\gamma = \frac{D_{lim,fl}}{D_{lim,TC}} = \frac{\xi_{TC}}{\xi_{fl}},$$

where D_{lim} is the limit of the rotational diffusion for full-length protein or TC domain. By inserting the relevant radia this ratio is measured to be $\gamma = 0.45$.

Therefore the fraction of time in the sliding mode can be calculated as:

$$f = D_{fl,exp}/(\gamma.D_{Cterm,exp}) = 1.4/(6.7 \times 0.45) = 0.46.$$

So p53 spends about half of the time in the sliding state and half in the recognition state. Because our estimate of the diffusion coefficient for the full-length p53 is biased toward higher end, provided estimate is an upper estimate (i.e., protein spends less than 45% in the sliding state)

Sliding length and search time. To measure the mean sliding distance and search time we use (12)

$$n = \sqrt{4D_{1D}/k_{off}},$$

where n is the number of base-pairs visited in each round of one-dimensional diffusion, D_{1D} is the measured diffusion coefficient of full-length p53 on DNA ($D_{1D} = 1.4 \times 10^6$ bp^2/seconds) (Table 1). The diffusion coefficient in cell nucleus is about five times smaller due to the higher viscosity of the nucleus (16). k_{off} is the dissociation rate of p53 from nonspecific DNA ($k_{off} = 0.4\ s^{-1}$) (17, 18). Therefore the number of base-pairs visited in each round of one-dimensional diffusion can be estimated as

$$n = \sqrt{4D_{1D}/k_{off}} = 2\sqrt{1.4 \times 10^6/5/0.4} = 1{,}700 \text{ bp}.$$

The total search time can be measured by

$$t_s = \frac{M}{n}\left(\frac{1}{k_{on}} + \frac{1}{k_{off}}\right),$$

where k_{on} is the association rate of full-length p53 to nonspecific DNA ($k_{on} = 0.12$–$0.3\ s^{-1}$) (17, 18) and M is the length of the genome ($M = 2 \times 3 \times 10^9$ bps) for human genome. The fraction of accessible DNA due to chromatinization is 1–5% (19). Therefore the total search time can be estimated as:

$$t_s = \frac{M}{n}\left(\frac{1}{k_{on}} + \frac{1}{k_{off}}\right) = \frac{6.10^6(0.01\text{–}0.05)}{1{,}700}\left(\frac{1}{0.12\text{–}0.3} + \frac{1}{0.4}\right)$$
$$= (20\text{–}200) \times 10^4 \text{ sec}$$

This result is for one copy of p53 per cell. However the copy number of p53 in nucleus is much higher and is estimated to be 500–5,000 (20, 21). The number of active p53 proteins increases at the presence of different stress types. We assume 1,000 as the number of activated p53 molecules in cell nucleus. The total search time

for a single site (e.g., p21 promoter) to be found by any p53 molecule is therefore:

$$t_s = (200\text{–}2{,}000)\ \text{sec} \approx 3\text{–}30\ \text{min}.$$

This estimate is consistent with p21 initial activation response of about 1 h.

In chromatinized DNA, then presence of nucleosomes can reduce the sliding distance to the size of the nucleosome-free region in the promoter ~500 bp. Then the entire search takes about $1{,}700/500 = 3.1$ fold longer.

The rate of the conformational transition. Efficient search requires that the cognate site is recognized at least once during a round of sliding. This requirement does not mean that the proteins shall undergo the conformational transition each time it visits every site. Each site is visited many ($\sim n$ times). It is imperative that the protein undergoes the conformational transition at least once during all the visits of a site, i.e., during an interval of time $\sim \tau_{1D}/n$:

$$\tau_{\text{residence}} \approx \frac{\tau_{1D}}{n} = \frac{1}{k_{\text{off}} n} = \frac{1}{0.4 \cdot 1{,}700} = 1.5\ \text{ms}.$$

Fast search if conformational transition takes less than residence time:

$$\tau_{\text{conf}} < \tau_{\text{residence}}.$$

The rate of the conformational transition from search state to recognition state k_{SR} (Fig. 4, main text) shall be greater then 700 s^{-1} , i.e., millisecond range, which is a very reasonable requirement even for such big tetramer as p53 (LacI was shown to undergo a transition in the submilisecond range). The transition from recognition state to search state, k_{RS} is determined by the stability of the complex of p53 and DNA.

1. Lee JB, et al. (2006) DNA primase acts as a molecular brake in DNA replication. *Nature* 439:621–624.
2. van Oijen AM, et al. (2003) Single-molecule kinetics of lambda exonuclease reveal base dependence and dynamic disorder. *Science* 301:1235–1238.
3. Tafvizi A, et al. (2008) Tumor suppressor p53 slides on DNA with low friction and high stability. *Biophys J* 95:L01–03.
4. Blainey PC, van Oijen AM, Banerjee A, Verdine GL, Xie XS (2006) A base-excision DNA-repair protein finds intrahelical lesion bases by fast sliding in contact with DNA. *Proc Natl Acad Sci USA* 103:5752–5757.
5. Natan E, Hirschberg D, Morgner N, Robinson CV, Fersht AR (2009) Ultraslow oligomerization equilibria of p53 and its implications. *Proc Natl Acad Sci USA* 106:14327–14332.
6. Weinberg RL, Freund SM, Veprintsev DB, Bycroft M, Fersht AR (2004) Regulation of DNA binding of p53 by its C-terminal domain. *J Mol Biol* 342:801–811.
7. Nikolova PV, Henckel J, Lane DP, Fersht AR (1998) Semirational design of active tumor suppressor p53 DNA-binding domain with enhanced stability. *Proc Natl Acad Sci USA* 95:14675–14680.
8. Veprintsev DB, et al. (2006) Core domain interactions in full-length p53 in solution. *Proc Natl Acad Sci USA* 103:2115–2119.
9. Kochaniak AB, et al. (2009) Proliferating cell nuclear antigen uses two distinct modes to move along DNA. *J Biol Chem* 284:17700–17710.
10. Kuhn H, Frank-Kamenetskii MD (2008) Labeling of unique sequences in double-stranded DNA at sites of vicinal nicks generated by nicking endonucleases. *Nucleic Acids Res* 36:e40.
11. Doyle PS, Ladoux B, Viovy JL (2000) Dynamics of a tethered polymer in shear flow. *Phys Rev Lett* 84:4769–4772.
12. Slutsky M, Mirny LA (2004) Kinetics of protein-DNA interaction: facilitated target location in sequence-dependent potential. *Biophys J* 87:4021–4035.
13. Ang HC, Joerger AC, Mayer S, Fersht AR (2006) Effects of common cancer mutations on stability and DNA binding of full-length p53 compared with isolated core domains. *J Biol Chem* 281:21934–21941.
14. Tidow H, et al. (2007) Quaternary structures of tumor suppressor p53 and a specific p53 DNA complex. *Proc Natl Acad Sci USA* 104:12324–12329.
15. Bagchi B, Blainey PC, Xie XS (2008) Diffusion constant of a nonspecifically bound protein undergoing curvilinear motion along DNA. *J Phys Chem B* 112:6282–6284.
16. Phair RD, Gorski SA, Misteli T (2004) Measurement of dynamic protein binding to chromatin in vivo, using photo-bleaching microscopy. *Methods Enzymol* 375:393–414.
17. Mueller F, Wach P, McNally JG (2008) Evidence for a common mode of transcription factor interaction with chromatin as revealed by improved quantitative fluorescence recovery after photobleaching. *Biophys J* 94:3323–3339.
18. Hinow P, et al. (2006) The DNA-binding activity of p53 displays reaction-diffusion kinetics. *Biophys J* 91:330–342.
19. Hesselberth JR, et al. (2009) Global mapping of protein-DNA interactions in vivo by digital genomic footprinting. *Nat Methods* 6:283–289.
20. Kuznetsov VA, Orlov YL, Wei CL, Ruan Y (2007) Computational analysis and modeling of genome-scale avidity distribution of transcription factor binding sites in chip-pet experiments. *Genome Inform* 19:83–94.
21. Wang YV, et al. (2007) Quantitative analyses reveal the importance of regulated Hdmx degradation for p53 activation. *Proc Natl Acad Sci USA* 104:12365–12370.

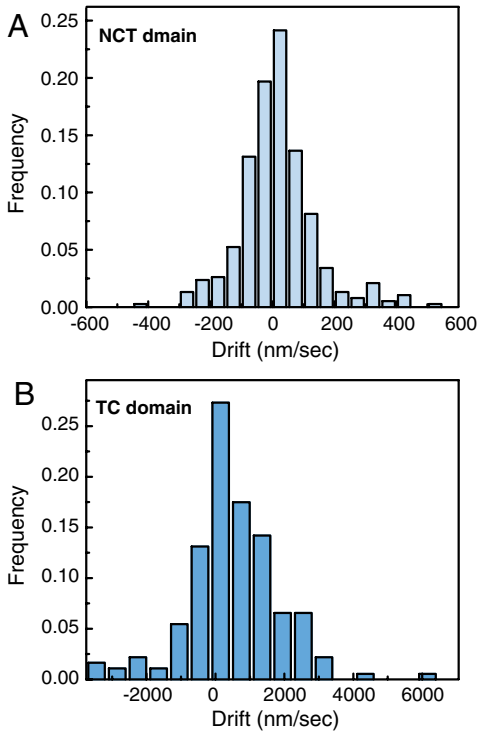

Fig. S1. Histogram of drift for different DNA-binding domains of p53. (*A*) Histogram of drift for 385 individual NCT trajectories. The drift for NCT domain is almost centered around zero, resulting in a small mean of 6.1 ± 7.6 nm/sec. (*B*) Histogram of drift for 183 individual TC domain trajectories. The weighted drift for TC domain is 355.8 ± 98.4 nm/seconds. Similar distribution of drift is observed for other salt concentrations.

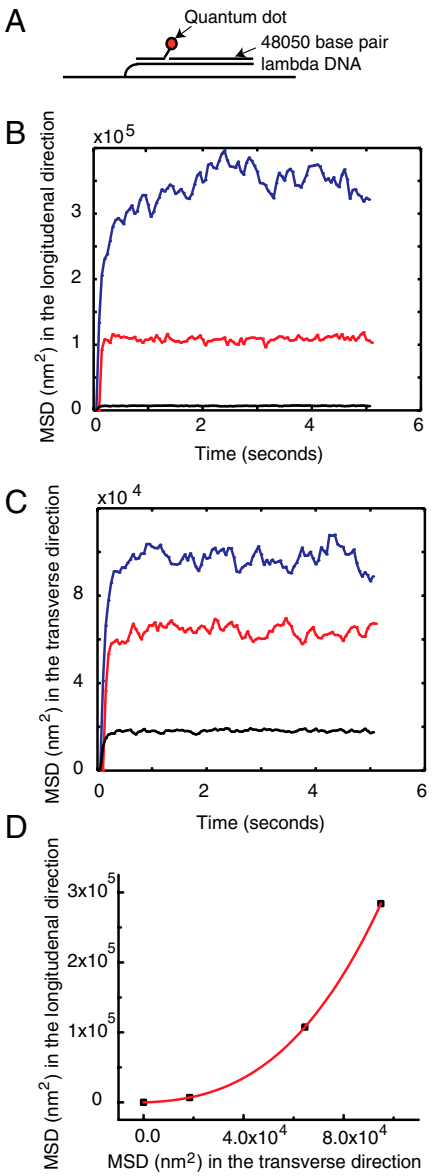

Fig. S2. Measurements of the Mean Square Displacements of DNA fluctuations. (*A*) The fluctuation of DNA due to Brownian motion can be measured by attaching a quantum dot to different locations along DNA. (*B*) MSD vs. time in the direction of the flow of quantum dots attached to 14,725 bp (black), 33,777 bp (red) and 48,502 bp (blue) on DNA. As can be seen from the graphs, the MSD of first two quantum dots doesn't increase after time = 0.25 seconds. (*C*) MSD vs. time in the direction transverse to the direction of the flow for the same quantum dots trajectories. (*D*) MSD of bound quantum dots in the longitudinal direction and transverse direction at time $t = 0.5$ seconds. Only trajectories with MSD less than 7×10^4 nm^2/seconds in the transverse direction are chosen to assure the minimal effect of DNA fluctuations in the longitudinal direction on measured diffusion coefficient.

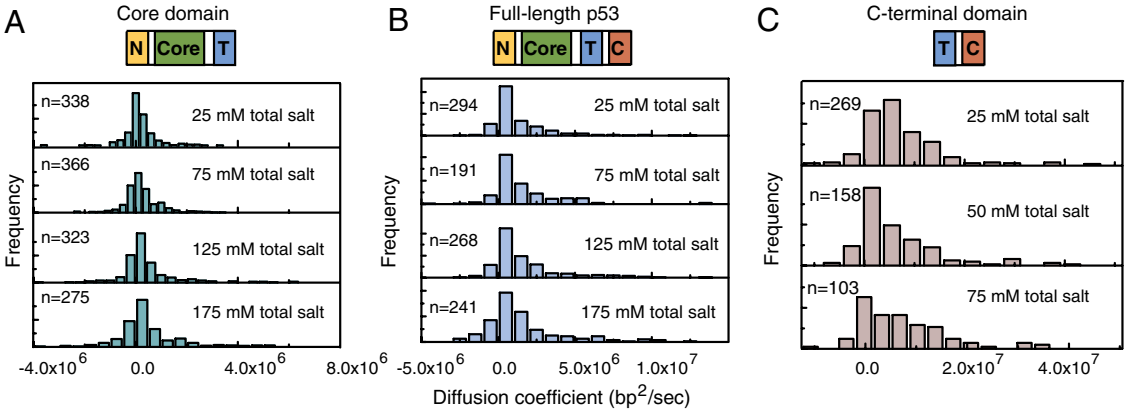

Fig. S3. Histogram of diffusion coefficient on DNA for different p53 constructs. (*A*) Histogram of diffusion coefficient of NCT in different total salt concentration; the number of trajectories *n* are noted in each histogram. (*B*) Histogram of diffusion coefficient of full-length p53 protein in different total salt concentration. (*C*) Histogram of diffusion coefficient of TC domain in different total salt concentration.

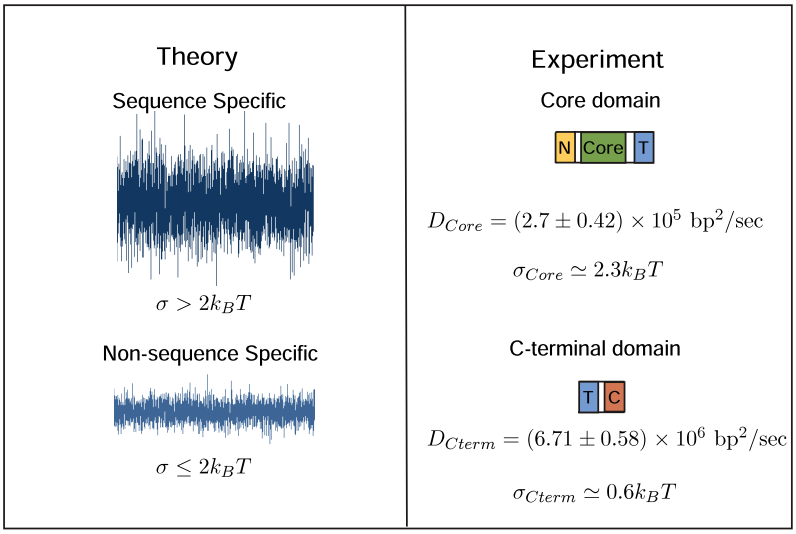

Fig. S4. Effect of the energy landscape on the rate of translocation of different DNA-binding domains: comparison of theoretical predictions and experimental observations. Sequence specificity of the protein-DNA interactions requires rough energy landscapes with large variance σ. The slow diffusion of the core domain, which is the sequence-specific domain of p53, is consistent with this theory and results in $\sigma = 2.3\ k_BT$. C-terminal domain on the other hand is nonsequence dependant and binds all DNA sequences. Theory suggests a small roughness of the energy landscape for such protein-DNA interactions. The fast translocation of the C-terminal domain on DNA is consistent with theory and results in $\sigma = 0.6\ k_BT$.

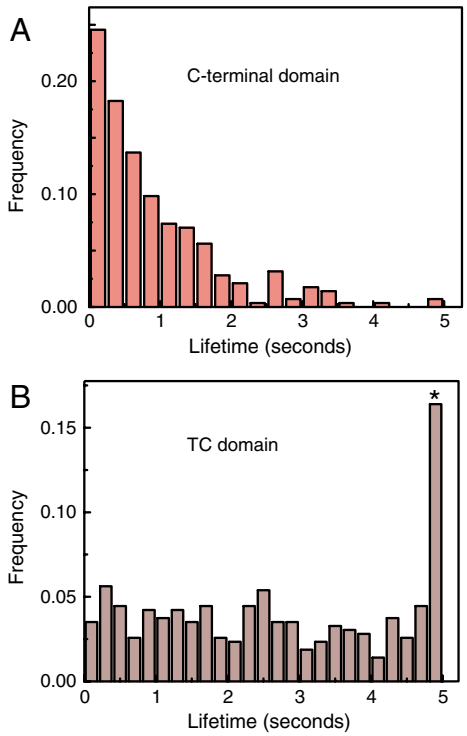

Fig. S5. Comparison of the lifetime of C-terminal domain and TC domain on DNA. (*A*) Histogram of lifetime of C-terminal domain on DNA for 285 individual trajectories in 25 mM total salt concentration. The average lifetime of C-terminal domain on DNA is 0.88 ± 0.05 seconds. (*B*) Histogram of lifetime of TC domain on DNA for 429 individual trajectories in 25 mM total salt concentration. The average lifetime of TC domain on DNA is 2.41 ± 0.08 seconds. Total acquisition time is 5 s. The asterisk indicates that the frequency shown represents lifetime for all values equal or greater than the indicated lifetime. The average lifetime of the TC domain is much larger than that of C-terminal domain alone. Because Tetramerization domain does not interact with DNA, this suggests that the TC domain in our experimental condition is oligomerized resulting in interactions of more than one C-terminal domain with DNA.

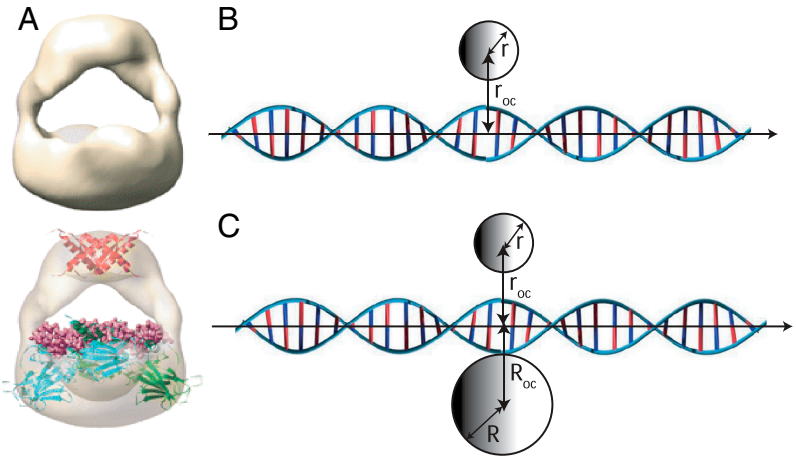

Fig. S6. The structure of p53 used in our model of p53 search on DNA. (*A*) The quaternary structure of p53 on the cognate DNA site by a combination of small-angle X-ray scattering and NMR (14). The structure shows that the core domains are in close contact with the DNA, while the tetramerization domains form the most remote region of the structure on the other side of DNA. The maximum theoretical diffusion coefficient with no energy barrier for TC domain (*B*) and full-length protein (*C*) can be calculated by rotational diffusion of the constructs along DNA.